

# Investigation of carbon nanotube sheet for lunar dust shielding

Volume 54: 1–16  
© The Author(s) 2024  
Article reuse guidelines:  
[sagepub.com/journals-permissions](https://sagepub.com/journals-permissions)  
DOI: 10.1177/15280837231224077  
[journals.sagepub.com/home/jit](https://journals.sagepub.com/home/jit)



Prakash Giri<sup>1</sup> , Shaaban Abdallah<sup>2</sup>, Woo Kyun Kim<sup>1</sup>,  
Noe T. Alvarez<sup>3</sup> and Mark Schulz<sup>1</sup>

## Abstract

Carbon nanotubes (CNT) sheet is a new type of nonwoven fabric that is being evaluated for different applications. This article presents the first friction-based investigation of the use of CNT sheet as a dust shield. The focus application is for shielding future machinery on the moon from lunar dust. Lunar dust is strongly abrasive; it adheres to all surfaces and causes wear. The absence of an atmosphere and water on the moon, along with its low gravity, and electrostatic adhesion exacerbates the issue of lunar dust, which affects all surfaces, including machinery and human apparel. Friction testing was performed to represent the effect of abrasion occurring on a garment surface while astronauts are working on the moon. The coefficients of static and sliding friction between two CNT sheets, held against each other by a weight, were 0.6 and 0.45, respectively. The presence of lunar regolith simulant reduced the friction coefficients between the two CNT sheets by 33% and 22% for static and sliding friction, respectively. The dust in the sheets was

<sup>1</sup>Department of Mechanical and Materials Engineering, CEAS, University of Cincinnati, Cincinnati, OH, USA

<sup>2</sup>Department of Aerospace Engineering & Engineering Mechanics, CEAS, University of Cincinnati, Cincinnati, OH, USA

<sup>3</sup>Department of Chemistry, University of Cincinnati, Cincinnati, OH, USA

## Corresponding authors:

Prakash Giri, Department of Mechanical and Materials Engineering, CEAS, University of Cincinnati, 2600 Clifton Ave, Cincinnati, OH 45221, USA.

Email: [giriph@mail.uc.edu](mailto:giriph@mail.uc.edu)

Mark Schulz, Department of Mechanical and Materials Engineering, CEAS, University of Cincinnati, 2600 Clifton Ave, Cincinnati, OH 45221, USA.

Email: [schulzmk@ucmail.uc.edu](mailto:schulzmk@ucmail.uc.edu)



Creative Commons Non Commercial CC BY-NC: This article is distributed under the terms of the Creative Commons Attribution-NonCommercial 4.0 License (<https://creativecommons.org/licenses/by-nc/4.0/>) which permits non-commercial use, reproduction and distribution of the work without further permission provided the original work is attributed as specified on the SAGE and Open Access pages (<https://us.sagepub.com/en-us/nam/open-access-at-sage>).

easily cleaned with dry wiping and compressed air, showing no requirement to use water for cleaning in space applications. However, the CNT sheets experienced wear after repeated friction tests. The CNT sheets passed the flammability test standards ASTM D6413/D6413M-15 and NPFA 1971 for applications under extreme heat conditions. Thus, CNT sheet can be considered as a multi-functional material for lunar applications, with shielding protection against dust and electromagnetic waves, and resistance to high temperatures.

## Keywords

Carbon nanotubes sheet, lunar dust, lunar textile, shielding

## Introduction

In the lunar environment dust collects on surfaces and causes friction and wear. This paper investigates if the use of carbon nanotube (CNT) sheet can reduce friction between surfaces. Simulated Lunar Highlands Dust (LHS-1D) obtained from Exolith Lab.<sup>1</sup> was used in the experiments. The goal of using CNT sheets was to reduce friction and wear on surfaces of equipment and machinery working on the moon. CNT sheets are useful in addressing three major problems reported regarding lunar dust: Dust Adhesion and Abrasion, Surface Electric Fields, and Dust Transport.<sup>2</sup> Researchers have shown CNT composites capability in radiation shielding such as proton radiation, electromagnetic radiation, and ultraviolet radiation, which is important for space applications.<sup>3-5</sup> CNT sheets are lightweight, they can be tailored for their stress-strain behavior (CNT composite sheets), they are conductive, and they are hydrophobic.<sup>6-8</sup> Hence, they can become a potential candidate for space exploration if they can withstand the extreme lunar dust environment consisting of strongly abrasive particles.

Lunar dust is reported to cause serious problems in space exploration. It can adhere to surfaces causing coating, contamination, false instrument readings, clogging, thermal and optical control problems, abrasion, equipment failure, and loss of traction.<sup>2,9-11</sup> Lunar dust can interfere with vision, and inhalation and irritation may occur.<sup>2,9</sup> Besides, lunar dust is found to be electrically charged which results in enhanced adhesion to clothing and equipment.<sup>2</sup> A text citing commander of Apollo 17, Eugene Cernan, states that “...one of the most aggravating, restricting facets of lunar surface exploration is the dust and its adherence to everything no matter what kind of material, whether it be skin, suit material, metal, no matter what it be and its restrictive friction-like action to everything it gets on”.<sup>2,12</sup> Electrically insulating materials and coatings are prone to charge buildup. The conductive properties of CNT sheet can reduce the problems relating to surface charge buildup and enhanced dust adhesion by providing electrostatic discharge.<sup>13</sup>

Researchers have considered many methods such as electrostatic repelling mechanisms, attraction mechanisms, and surface treatment methods to eliminate

lunar dust problems.<sup>14–16</sup> Metals and oxides have also been tested.<sup>17</sup> Different mechanisms such as diffusion, inertial impaction, interception, and electrostatic attraction act together for efficient filtration of particles.<sup>18–20</sup> Lunar dust particles can be studied to obtain their powder size distribution, so that the dominating mechanism for filtration can be determined. Then CNT membranes can be tailored in terms of diameter, porosity, and permeability to obtain good filtration efficiency. Some researchers have already studied CNT as a potential member to filter lunar dust reaching sensitive machinery and equipment, while others have experimented with the use of CNT in spacesuits for dust mitigation.<sup>16,21,22</sup> Though the use of CNT as a filter membrane has been studied, the use of CNT as a lunar surface textile still remains underrepresented.

The progress in the development of macroscale CNT composites has provided us with an opportunity to expand its use to shielding, conducting, and structural support applications along with filtration. However, the study of innovative CNT films and CNT composite sheets needs to be explored further to develop reliable dust mitigation solutions. This study presents preliminary results on the fabrication of macroscale CNT sheet using a customizable synthesis process. We have investigated the electrical conductivity, flame resistance, and studied the potential use of CNT sheet as a surface textile material to withstand extreme lunar dust conditions in absence of water as a cleaning medium. The frictional interaction between CNT and lunar dust is studied in this paper so the “...restrictive friction-like action to everything...” problem as stated by Eugene Cernan can be addressed.

## Synthesis of carbon nanotubes sheet

The synthesis of pristine CNT sheet was performed on a horizontal Floating Catalyst Chemical Vapor Deposition (FC-CVD) reactor, using a fuel consisting of methanol (100%, Fisher Chemical), ferrocene (98%, Fisher Chemical), n-hexane (99.9%, Lab. Alley) and thiophene ( $\geq 99\%$ , Aldrich Chemistry). The fuel was fed to the reactor through an atomizer at a rate of 80 mL/hr., using a syringe pump. An argon and hydrogen gas mixture is fed into the inlet of the reactor to disperse the catalyst and fuel particles and to carry the CNT through the reactor tube to the glove box. The temperature of the reactor was maintained at 1250°C during the synthesis. A CNT sock (web of CNT) coming out of the FC-CVD reactor was collected in a drum located at a distance of 5 cm from reactor outlet and rotating at 4.3 RPM. An inert atmosphere of Argon was maintained inside a glove box for the synthesis process. A smooth film of CNT sheet was produced over time and acetone was used to densify the collected CNT sock. Pristine sock coming out of the reactor was collected on a rotating and translating drum. As a layer of sock covered the collector surface, acetone was sprayed for densification. The schematics of the synthesis process and image of a CNT sheet thus produced are presented in [Figure 1\(a\)](#) and [\(b\)](#) respectively.

The synthesis process is scalable. The dimensions of the CNT sheets can be altered by changing the collector drum diameter and translational distance. The fuel feed rate and

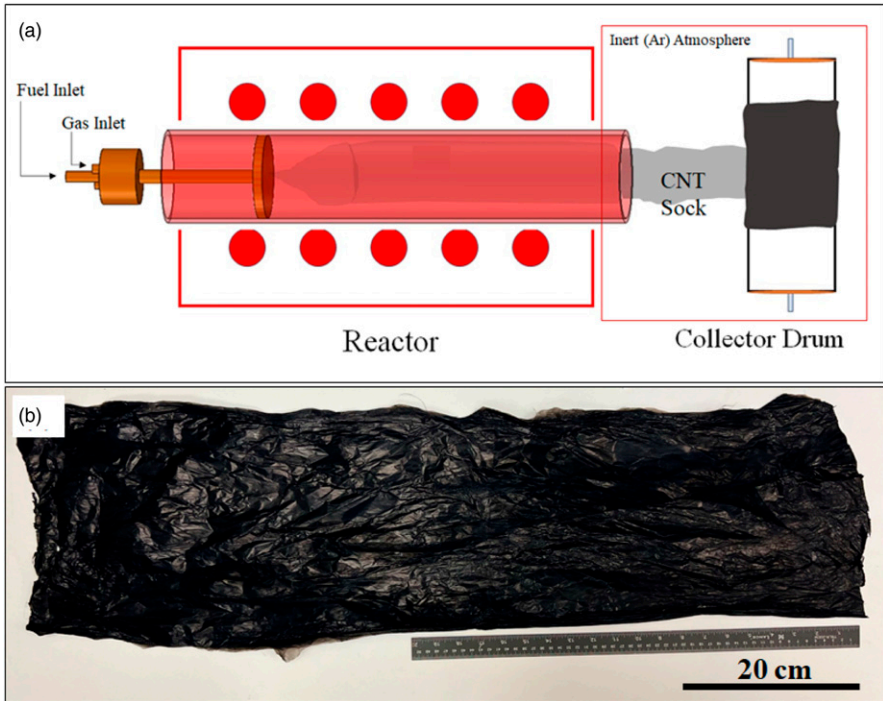


**Figure 1.** Overview of CNT sheet synthesis. (a) Schematics of CNT synthesis using horizontal FC-CVD, (b) CNT sheet synthesized using the FC-CVD reactor.

duration help to control the thickness of the CNT sheet. More details about CNT sheet manufacturing will be available after a patenting process is completed.

## Properties of carbon nanotubes sheet

The laboratory arrangement of CNT sock collection for formation of macroscale CNT sheet is shown in [Figure 2\(a\)](#). The pristine CNT sheet size fabricated for our test was 25 cm by 90 cm with a thickness of 20 microns. The density of the sheet was 0.25 g/cc. The sheet was electrically conductive with a resistivity of 0.0043  $\Omega\cdot\text{cm}$  along length (synthesis direction), and 0.0091  $\Omega\cdot\text{cm}$  along the width. The measurement was made using a two-point method as shown in [Figure 2\(b\)](#).<sup>23</sup> The difference in resistivity along length and width arose due to the anisotropy in CNT sheet induced during sock collection.<sup>24</sup> The electrical resistance of the sheet is much greater through the thickness of the sheet than in-plane. The greater resistance through the thickness is due to the greater number of nanotube-to-nanotube lateral junctions. The junctions are expected to have higher resistance to electron flow than the nanotube walls.<sup>25</sup> The conductivity anisotropy ratio  $k^{\parallel}/k^{\perp}$  in plane was calculated to be 2.12. The resistivity was also measured using a

contactless surface resistivity measurement method (Delcom Instruments Inc. 873 Interface Module) and was found to be in a similar range ( $0.004 \Omega \cdot \text{cm}$ ). Surface resistivity was multiplied by thickness of the sheet to determine its bulk volumetric resistivity (by the instrument). The two-point method measures resistivity along the synthesis direction and perpendicular direction, whereas the surface resistivity method measures average surface resistivity. The lower the electrical resistance, the better CNT sheet will shield electromagnetic waves and discharge static electricity.

SEM imaging (FEI Aprio LV-SEM) of the CNT sheet is presented in Figure 3(a). The CNT membrane consisted of strands of CNTs with diameters ranging from 4.47 nm to 38.38 nm. Figure 3(b) presents the diameter distribution of the CNT fibers in the CNT sheet.

The CNT sheets were thermally and electrically conductive and passed flammability test standard ASTM D6413/D6413M-15.<sup>26,27</sup> Details about the flame test are as presented in Table 1.



**Figure 2.** Electrical characterization of CNT sheet. (a) Collection of CNT sock to form CNT sheet, (b) Resistivity measurement using two-point method, (c) Contactless resistivity measurement.

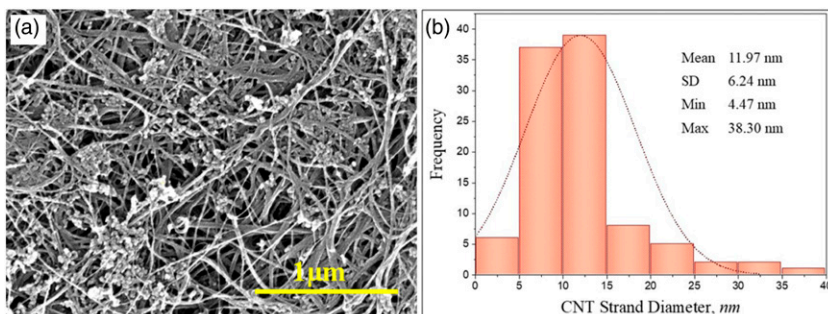


**Figure 3.** Characterizing CNT strands. (a) SEM image of CNT sheet, (b) CNT strands diameter distribution.

The after-flame time, after-glow time and char length were within the limits of the flammability test standard. There was no melting and dripping of the CNT sheet (Figure 4).

The CNT sheets were also placed in an oven at 260°C for 5 min. The sheets remained intact without melting, dripping, or shrinking, thus showing compatibility with NPFA 1971 (Forced Air Oven Test) (Figure 5).

The tensile strength of the CNT sheets was measured using Micro Instron Testing Machine, Model 5948. A gauge length of 20 mm and width of 2 mm was maintained for the sample specimens. The specimens were supported with the help of a rectangular paper specimen holder. Pneumatic grips were used for the tests.

The length direction of the CNT sheet is considered as the dimension across the rolling (sock collection) direction, whereas the width direction is considered to be perpendicular to the direction of sock collection. Along length the elastic limit is  $\sim 7$  MPa and the sheet fails after withstanding a stress of  $\sim 28$  MPa and around 26% strain. Whereas the elastic limit along the width is  $\sim 3.5$  MPa and the sheet fails at  $\sim 12$  MPa at around 55% strain (Figure 6). This peculiar behavior of failing at nearly half the stress but double the strain arises from the anisotropy in the CNT sheets, as discussed earlier. In nonwoven CNT

**Table I.** Flame retardancy test parameters and observed results.

Flame application time(secs)	After-flame time(second)	Afterglow time(second)	Char length(cm)	Melting /Dripping
12	<1	<1	<4	Not observed

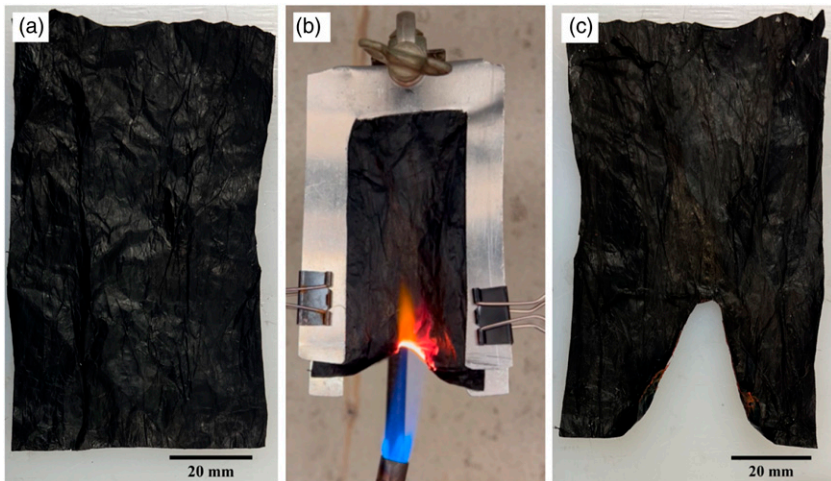


**Figure 4.** Pristine CNT Sheet (a) before flame test, (b) during flame test, and (c) after flame test.

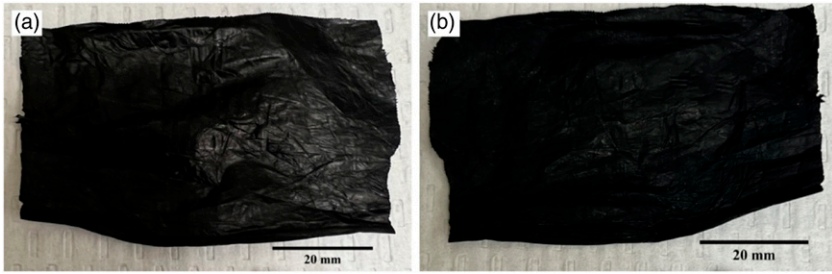


**Figure 5.** Pristine CNT sheets (a) before the forced air oven test, and (b) after the forced air oven test.

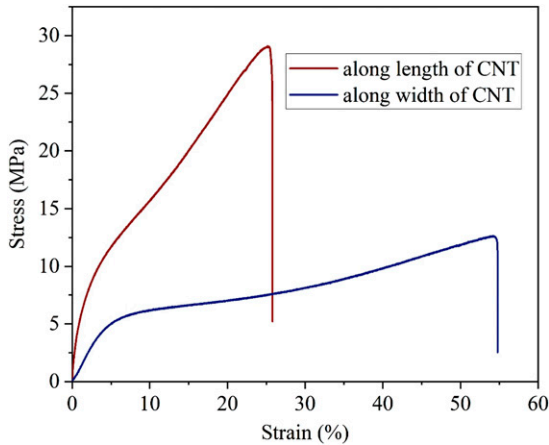


**Figure 6.** Stress-strain behavior of CNT sheet along length and width.

sheet, the nanotube strands are randomly oriented and under external stress the strands slip apart. The individual nanotubes do not break. Thus, the strength of CNT fabric is low but the strain to failure is large. In the sheet winding direction, the CNT strands or bundles of nanotubes partially align and make the fabric stronger in this direction. In the sheet width direction, the nanotube strands are not aligned and the strength is lower but the strain to failure is larger.

## Properties of particles tested

Properties of the Lunar Regolith Simulant particles used in the testing, as provided by the supplier are given in [Table 2](#).<sup>1</sup>

The SEM imaging (FEI Aprio LV-SEM) of the Lunar Regolith Simulant is presented in [Figure 7](#). The Lunar Regolith Simulant tends to agglomerate randomly and show an inhomogeneous size distribution.

Tin (Sn) nanoparticles, SAE 20 oil and de-ionized water were also tested for relative comparison with Lunar Regolith Simulant in the friction test. Sn nanoparticles were obtained from SkySpring Nanomaterials Inc. The particle size ranged from 10 nm to 80 nm, and is supposed to act as a lubricant, filling in scratches and worn surfaces, thus minimizing friction in the surfaces.

## Results and discussion

Lunar Regolith Simulant from the Exolith Lab. was used to study the corroding and sticking interactions with CNT sheet. A section of pristine CNT sheet as shown in [Figure 8\(a\)](#) was taken and 5 grams of Lunar Regolith Simulant was sprayed on the top as shown in [Figure 8\(b\)](#). The Lunar Regolith Simulant was allowed to sit on the sheet for

**Table 2.** Properties of lunar regolith simulant.

Mean particle size	7 $\mu\text{m}$ (<4 $\mu\text{m}$ - 35 $\mu\text{m}$ range)
Uncompressed bulk density	0.07 $\text{g}/\text{cm}^3$
Constituents (minerology)	Anorthosite, glass-rich basalt, ilmenite, olivine, pyroxene
Constituents (oxides)	$\text{SiO}_2$ , $\text{TiO}_2$ , $\text{Al}_2\text{O}_3$ , $\text{FeO}$ , $\text{MnO}$ , $\text{MgO}$ , $\text{CaO}$ , $\text{Na}_2\text{O}$ , $\text{K}_2\text{O}$ , $\text{P}_2\text{O}_5$
Constituents (trace elements)	Ni, Cr, V, Sc, Cu, Zn, Ga, Ba, Rb, Cs, Sr., Y, Zr, Hf, Nb, Ta, Mo, La, Ce, Nd, Sm, Dy, Yb, Th, U, Tl, Pb, Sn, Bi, Sb
Constituents (volatiles)	F, Cl, $\text{SO}_3$ , Br, As

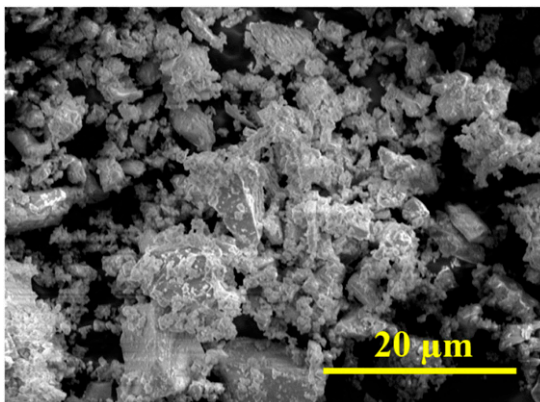


**Figure 7.** SEM of lunar regolith simulant.

5 min. No external pressure was applied, and the Lunar Regolith Simulant was allowed to fall freely from the pristine sheet. 4.9990 grams of the Lunar Regolith Simulant was recovered back. 0.0008 g of the Regolith was found to have been stuck in the pristine sheet, and 0.0002 g remained unaccounted (lost) during the experiment. Part of unaccounted amount of Lunar Dust Regolith was expected to enter the inherent pores in CNT materials, but it remained undetected in SEM imaging of the CNT sheet after the experiment. It was qualitatively seen that the Lunar Regolith Simulant does not readily stick to pristine CNT sheet without external force/pressure. The pristine sheet at the end of the experiment is shown in [Figure 8\(c\)](#).

The sticking nature of Lunar Regolith Simulant was further investigated by spreading the simulant particles on the CNT sheet and cleaning with compressed air. Air flowing at a velocity of 1 m/s was blown through a nozzle diameter of 3 mm to clean the CNT sheet.

The smooth CNT surface at the nanoscale may be a reason why dust particles do not adhere well to the CNT sheet. As CNT sheets are electrically conductive, they tend to distribute the electrostatic charge buildup over their surface which could quickly dissipate. As a result, CNT sheet that is not charged does not support electrostatic adhesion and thus has less affinity for dust particles.

The interaction of Lunar Regolith Simulant with CNT sheet along with external force was studied with the use of a simple force gauge. This friction test was conducted with an external pressure under a normal force load to represent light compaction of garments that could occur in use. A pristine sheet was fixed on top of a Teflon base as shown in [Figure 9\(a\)](#). An iron slider block was covered by another layer of pristine sheet. The block system weighing 10 N was connected to a spring scale as shown. This block system acts as an external pressure.

The block covered in pristine sheet was placed on top of the fixed sheet and pulled from the free end of the spring scale to measure the static friction force. The sliding friction force was measured by reading the spring scale while sliding the block on the fixed sheet. The sliding started outside the fixed sheet, in the Teflon block, and slid through the fixed sheet.

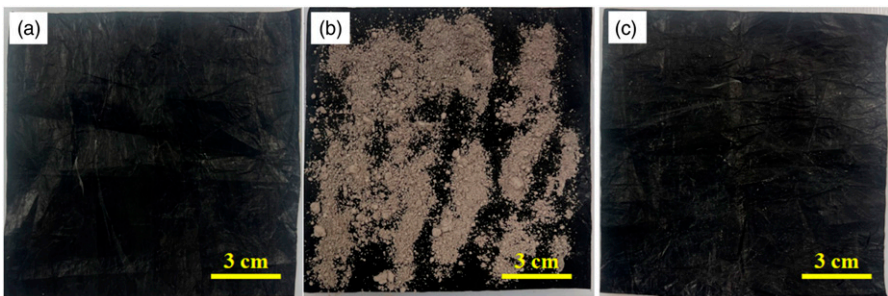


**Figure 8.** CNT sheet and lunar regolith testing. (a) Pristine CNT sheet, (b) Lunar regolith simulant sprayed on top of the sheet, (c) Lunar regolith simulant allowed to slide away from the sheet.

Observations were made for contact between two pristine CNT sheets. Similar observations were repeated by placing samples of Lunar Regolith Simulant, Tin (Sn) nanoparticles, SAE 20 oil and de-ionized water as lubricating materials in between two pristine sheets for relative comparison. CNT sheets as synthesized are hydrophobic but oleophilic, [Figure 9\(b\) and \(c\)](#). The lotus effect and non-polar structure of the CNTs attributed to their hydrophobic and oleophilic nature.<sup>28,29</sup> The coefficient of friction  $\mu$  was calculated as  $\mu = f(N)/W(N)$  where  $f$  is the force measured using the spring scale and  $W$  is the weight of the block both in the units of Newtons.<sup>30</sup> The coefficients of friction calculated between the two CNT surfaces with different materials sandwiched in between are listed in [Table 3](#).

The use of the Lunar Regolith Simulant, Sn nanoparticles, Oil and water film reduced the friction coefficient between two pristine sheets. Pristine CNT sheets without any intermediate materials lasted for 3 test cycles before tearing. When Dust and Sn nanoparticles were used, the CNT sheets lasted for 5 test cycles before showing significant rupture. The sheets lasted for 8 test cycles when water was used as a lubricating medium. Interestingly, the sheets lasted for a greater number of sliding tests with oil than any other materials although we experienced occasional interruption in our tests due to the sheets being adhered with each other. The pressure applied in the tests was 1762 Pascals (10 N weight on an area of  $5.68 \times 10^{-3} \text{ m}^2$ ). [Figure 10\(a\)–\(c\)](#) shows the

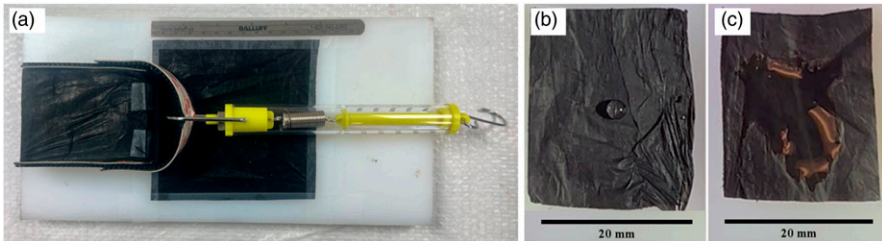


**Figure 9.** Test bed for friction testing. (a) Experimental setup for the friction test, (b) Hydrophobic and (c) Oleophilic nature of CNT membranes.

**Table 3.** Coefficients of friction for CNT sheets.

S. No.	Lubricating item	Static coeff. Of friction	Sliding coeff. Of friction
1	None	0.6	0.45
2	Lunar regolith simulant	0.4	0.35
3	Sn nanoparticles	0.45	0.42
4	SAE 20 oil	0.15 <sup>a</sup>	0.12
5	Water film (wet sheets)	0.4	0.35

<sup>a</sup>The CNT sheets stuck with each other occasionally due to the adhesion of oil during this test. The values obtained were discarded when the sheets were stuck to each other

tests using lunar dust, tin nanoparticles, and rupture initiation in the CNT sheet during the experiment.

The life of the CNT sheets also depended upon the surface conditions (for example: some CNT strands protruding from the sheets induced early rupture. This indicates the importance of the quality and surface finish of the sheets manufactured.). The CNT sheets had a muddy appearance with lunar dust when friction and pressure was applied. They were easily wiped clean with the help of a paper towel. They were also cleaned by using a compressed air gun (1 m/s air from a nozzle of 3 mm diameter). The results were similar to [Figures 8\(c\)](#) and [11\(c\)](#). The friction tests were repeated in a small vacuum (−2 inches of water) inside a glove box. The results were the same as before.

The smooth and strong nanostructured surface, and the hydrophobic nature of CNTs have contributed to resisting friction from surfaces. Moreover, the ability of CNT nonwoven sheet to endure large frictional forces comes from nanoscale interactions where the CNTs have the freedom to deform and slip over each other.<sup>31</sup>

CNT sheets before and after lunar dust testing were characterized using scanning electron microscopy (SEM) imaging to observe relative differences at the microscale. However, no noticeable differences were present. The white spots in the images are the result of some impurities attached to the sheets due to the handling and transfer of the sheets. ([Figure 12](#)).

A Renishaw inVia Raman spectroscope with a 514 nm laser was used to analyze the samples before and after the lunar dust test. A laser spot size of  $\sim 1 \mu\text{m}^2$  with a lens of 50x magnification was used with exposure time of 10 s for 3 accumulations. The overlaid

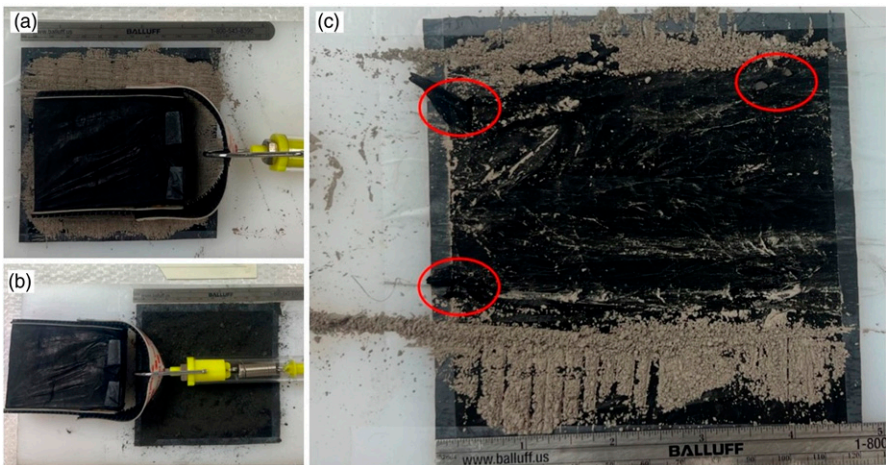


**Figure 10.** Measuring friction between two CNT sheets with particles between the sheets. (a) Test with simulated lunar regolith simulant; (b) Test with Sn nanoparticles; (c) Initiation of rupture after a few tests.

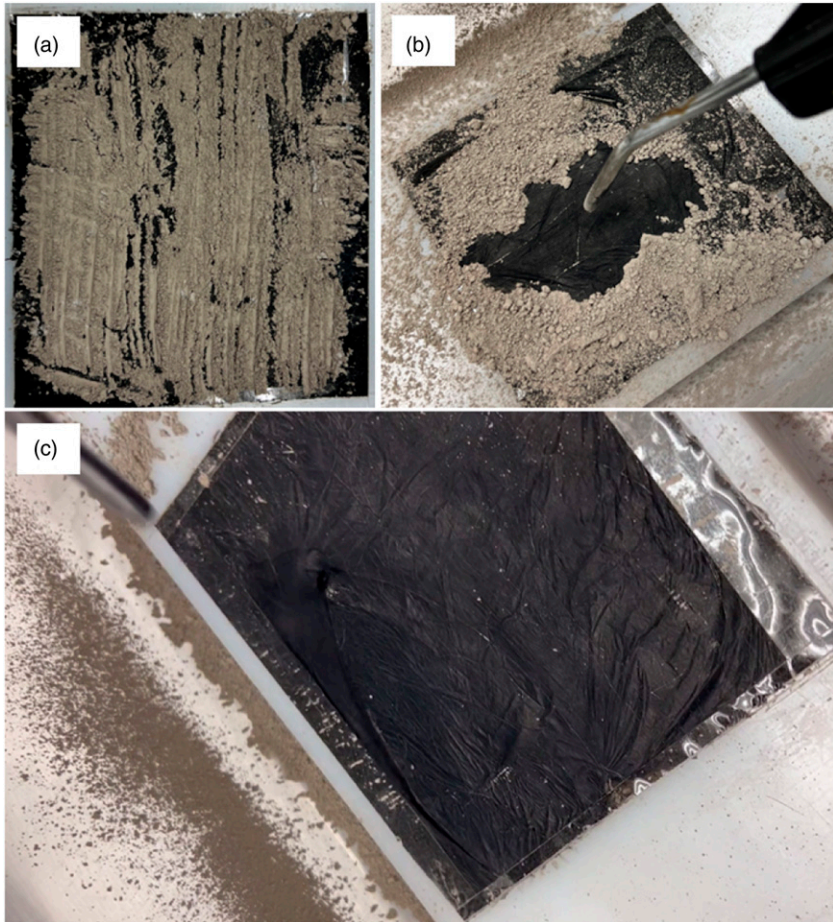


**Figure 11.** Interaction of CNT sheet and lunar regolith. (a) Lunar regolith simulant sprayed on a CNT sheet, (b) Compressed air from nozzle being used to blow away the dust particles, (c) CNT sheet after blowing the dust particles. Notice in part (c), the dust did not stick to the CNT sheet but adhered to the surroundings (plastic box on which the system was placed). This shows lunar dust does not have an affinity to adhere to CNT sheet as it has with other materials.

Raman spectra of CNT sheet before and after lunar dust tests are shown in [Figure 13](#). Both the spectra show the D, G and 2D peaks which are the signature peaks of Carbon Nanotubes. There was no change in the vibrational behavior of the CNT sheet after the lunar dust test.

The SEM imaging and Raman spectra denoted no significant changes in the nanoscale properties of the CNT sheet after the lunar dust testing. This implies that CNT sheets can

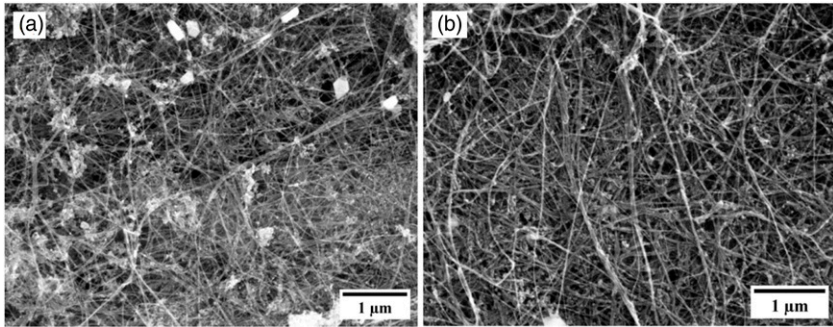


**Figure 12.** SEM imaging of CNT sheet (a) before lunar dust test, and (b) after lunar dust test.

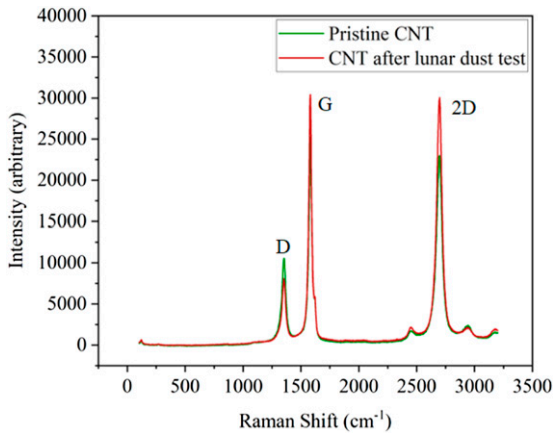


**Figure 13.** Raman spectra of pristine CNT and the CNT after the lunar dust test.

be used continuously in a lunar dust environment without degradation when mechanical wear and tear are prevented.

## Conclusions and suggested future work

The experiment shows that the CNT sheet to sheet dry static friction coefficient is in the range of 0.6. Adding Lunar Regolith Simulant particles to the sheet reduces the friction coefficient instead of raising it. The sheets tear after a few cycles, but they show positive results in terms of low frictional effects with simulant particles, and low adhesion of the particles on the surface. The sheets lasted longer with oil and water as a lubricating medium, indicating that some type of lubricating medium may be helpful in the lunar environment. The decrease in friction between two pristine sheets with the use of Lunar

Regolith Simulant as an intermediate material can signify that CNT sheets are more resistant to the frictional nature of the regolith simulant. The sheets after each test with Lunar Regolith Simulant were wiped off with a dry paper towel, and the sheets released the Lunar Regolith Simulant particles easily without sticking. Similar observations were made with compressed air. This testing of Lunar Regolith Simulants and CNT interactions shows an opportunity to use CNT sheets as lunar textiles. Considering the mix of properties including low density, good conductivity, high temperature resistance, high toughness and dust shielding, the study on macroscale CNT sheets needs to be expanded to comprehensively evaluate their application in space exploration. The frictional effects and flame resistance properties of CNT sheets combined with their electrical conductivity, radiation shielding capabilities, and mechanical strength demonstrates their potential as innovative multifunctional lunar textile materials, in addition to their potential application in space exploration activities.

Limitations of this study are that the Lunar Regolith's real morphology might be different on various environments of the lunar surface than the simulant material used in this study. Furthermore, the lunar conditions in which the particles acquire their electric charge are not exactly reproducible for our study on earth. Therefore, the adhesion properties described due to particle's morphology and electrostatic effects may not be an exact representation of the lunar environment.

The following future work is suggested: Bond CNT sheets to surfaces to prevent or reduce tearing of the sheet and develop CNT composite (layered) sheets to increase the strength of CNT sheets to use as a multifunctional structural component.

### Declaration of conflicting interests

The author(s) declared no potential conflicts of interest with respect to the research, authorship, and/or publication of this article.

### Funding

The author(s) disclosed receipt of the following financial support for the research, authorship, and/or publication of this article: This work was partially sponsored by the Ohio Workplace Safety Innovation Center Grant WSIC23-220513-010. This research study was also partly supported by the National Institute for Occupational Safety and Health through the Pilot Research Project Training Program of the University of Cincinnati Education and Research Center Grant T42OH008432.

### ORCID iD

Prakash Giri  <https://orcid.org/0000-0002-5550-3997>

### References

1. Exolith Lab. 2023. "Regolith simulants—Exolith lab." Accessed May 18, 2023. <https://exolithsimulants.com/collections/regolith-simulants>.
2. Stubbs TJ, Vondrak RR and Farrell WM. Impact of dust on lunar exploration. *Dust in planetary systems* Jan 2007; 643: 239–243.

3. Li Z, Nambiar S, Zheng W, et al. PDMS/single-walled carbon nanotube composite for proton radiation shielding in space applications. *Mater Lett* 1 Oct 2013; 108: 79–83.
4. Wang H, Wang G, Li W, et al. A material with high electromagnetic radiation shielding effectiveness fabricated using multi-walled carbon nanotubes wrapped with poly (ether sulfone) in a poly (ether ether ketone) matrix. *J Mater Chem* 2012; 22(39): 21232–21237.
5. Jagadeshvaran PL, Panwar K, Ramakrishnan I, et al. Smart textiles coated with functional particles derived from sustainable sources that can block both UV and EM. *Prog Org Coating* 1 Oct 2021; 159: 106404.
6. De Volder MF, Tawfick SH, Baughman RH, et al. Carbon nanotubes: present and future commercial applications. *Science* 1 Feb 2013; 339(6119): 535–539.
7. Wang K, Luo S, Wu Y, et al. Super-aligned carbon nanotube films as current collectors for lightweight and flexible lithium ion batteries. *Adv Funct Mater* 18 Feb 2013; 23(7):846–853.
8. Lee CH, Johnson N, Drelich J, et al. The performance of superhydrophobic and superoleophilic carbon nanotube meshes in water–oil filtration. *Carbon* 2011; 49(2): 669–676.
9. Gaier JR. *The effects of lunar dust on EVA systems during the Apollo missions*. Washington, DC: NASA, 2007.
10. Taylor L, Schmittm HH, Carrier WD, et al. Lunar dust problem: from liability to asset. In: 1st space exploration conference: continuing the voyage of discovery, Orlando, Florida, 30 January–01 February, 2005, 2005.
11. Bühler CA. Experimental investigation of lunar dust impact wear. *Wear* 2015; 342: 244–251.
12. Goodwin R, “Apollo 17: The NASA Mission Reports, vol. 1.” 2002.
13. Christensen G, Lou D, Grablander T, et al. Conductive coatings eliminate static discharge risk on aircraft. *TechConnect Briefs*. TechConnect.org, 2021.
14. Adams JG, Cline BL, Contaxes NA, et al. Lunar dust degradation effects and removal/prevention concepts. volume 1-summary final report. *Tech. Rep.* NASA, 1967.
15. Wohl CJ, Belcher MA, Hopkins JW, et al. Topographical modification of materials for lunar dust adhesion mitigation. In: 40th annual lunar and planetary science conference, The Woodlands, Mar 23–27, 2009.
16. Kruzelecky R, Wong B, Aissa B, et al. MoonDust lunar dust simulation and mitigation. In: 40th International Conference on Environmental Systems, Barcelona, Spain, 11–15 July 2010.
17. Matsumoto K, Suzuki M, Nishida SI, et al. Wear of materials in lunar dust environment. In: Proceedings of the 11th international symposium on materials in a space environment, Aix-en-Provence, France, 15–18 September 2009.
18. Giri P, Kakoria A, Verma S, et al. Nanofibers for sustainable filtration: a waste to energy approach. In: *Machines, Mechanism and Robotics: Proceedings of iNaCoMM 2019*. The Gateway: Springer Singapore, 2022, pp. 1693–1701.
19. Zhu M, Han J, Wang F, et al. Electrospun nanofibers membranes for effective air filtration. *Macromol Mater Eng* 2017; 302(1): 1600353.
20. Wen D, Jianhui W, Bing P, et al. An improved theoretical model of cigarette smoke filtration across mono-segment cellulose acetate filters. *Contributions to Tobacco & Nicotine Research* 2015; 26(5): 232–240.
21. Agui JH and Stocker DP. *NASA lunar dust filtration and separations workshop report*. Scotts Valley, CA: CreateSpace Independent Publishing Platform, 2009.

22. Manyapu KK, De Leon P, Peltz L, et al. Proof of concept demonstration of novel technologies for lunar spacesuit dust mitigation. *Acta Astronaut* 1 Aug 2017; 137: 472–481.
23. Heaney MB. Electrical conductivity and resistivity. In: *Electrical measurement, signal processing, and displays*. Boca Raton, FL: CRC Press, 2003, Vol. 7.
24. Sehrawat M, Rani M and Singh BP. One step fabrication of aligned carbon nanotube sheet via FC-cvd technique. *J Nanomater* 16 Jul 2022; 2022: 8318217.
25. Ward JW, Nichols J, Stachowiak TB, et al. Reduction of CNT interconnect resistance for the replacement of Cu for future technology nodes. *IEEE Trans Nanotechnol* 5 May 2011; 11(1): 56–62.
26. ASTM D6413/D6413M-15. *Standard test method for flame resistance of textiles (vertical test)*. West Conshohocken, PA: ASTM. Available online. <https://www.astm.org/Standards/D6413.htm> (accessed on 18 May 2023).
27. Magovac E, Vončina B, Budimir A, et al. Environmentally benign phytic acid-based nano-coating for multifunctional flame-retardant/antibacterial cotton. *Fibers* Nov 2021; 9(11): 69.
28. Liu Y, Tang J, Wang R, et al. Artificial lotus leaf structures from assembling carbon nanotubes and their applications in hydrophobic textiles. *J Mater Chem* 2007; 17(11): 1071–1078.
29. Kukkar D, Rani A, Kumar V, et al. Recent advances in carbon nanotube sponge-based sorption technologies for mitigation of marine oil spills. *J Colloid Interface Sci* 2020; 570: 411–422.
30. Burwell JT and Rabinowicz E. The nature of the coefficient of friction. *J Appl Phys* Feb 1953; 24(2): 136–139.
31. Heo SJ and Susan B. Sinnott. “Effect of molecular interactions on carbon nanotube friction”. *J Appl Phys* 2007; 102: 6.